Temperature dependence of interlayer magnetoresistance in anisotropic layered metals

Braden A. W. Brinkman and Malcolm P. Kennett
Department of Physics, Simon Fraser University, 8888 University Drive, Burnaby, British Columbia, Canada V5A 1S6
(Received 26 November 2008; revised manuscript received 13 August 2009; published 4 September 2009)

Studies of interlayer transport in layered metals have generally made use of zero-temperature conductivity expressions to analyze angle-dependent magnetoresistance oscillations (AMRO). However, recent high temperature AMRO experiments have been performed in a regime where the inclusion of finite temperature effects may be required for a quantitative description of the resistivity. We calculate the interlayer conductivity in layered metals with isotropic and anisotropic Fermi surface properties allowing for finite temperature effects. We find that resistance maxima are modified by thermal effects much more strongly than resistance minima. We also use our expressions to calculate the interlayer resistivity appropriate to recent AMRO experiments in an overdoped cuprate which led to the conclusion that there is an anisotropic, linear in temperature contribution to the scattering rate and find that this conclusion is robust.

DOI: 10.1103/PhysRevB.80.094505 PACS number(s): 74.72.−h, 71.18.+y, 72.10.−d, 72.15.−v

I. INTRODUCTION

Angle-dependent magnetoresistance oscillations (AMRO) in the interlayer resistance of layered metals provide a means to determine Fermi surface properties of such systems.[1] Maps of two and three dimensional Fermi surfaces have been determined for a wide variety of materials.[2–7] AMRO can also be used to infer information about possible anisotropies in the momentum space of Fermi surface properties such as the scattering rate.[8–16] In particular, recent AMRO experiments by Abdel-Jawad *et al.*[9] reveal that in the overdoped cuprate $Tl_2Ba_2CuO_{6+\delta}$ (Tl2201) the scattering rate contains an anisotropic piece that varies with the same symmetry as the superconducting gap and grows linearly with temperature. The measured anisotropy in the scattering rate may have relevance to the origin of high temperature superconductivity in cuprate superconductors, as the strength of the anisotropic piece of the scattering increases with the critical temperature, T_c.[11] Scattering rate anisotropy has been detected in several other cuprates using angle-resolved photoemission spectroscopy (ARPES),[17–20] optical conductivity[21] and in-plane transport measurements.[22] Theoretical support for such anisotropic scattering comes from ideas about hot and cold spots on the Fermi surface, first raised in the context of optical conductivity,[23] and appears to arise naturally in dynamical mean field[24] and functional renormalization group[25] calculations on the two-dimensional Hubbard model.

An advantage of AMRO over other techniques which use oscillations to obtain information about the Fermi surface, such as de Haas–van Alphen and Shubnikov–de Haas oscillations, is that they can be measured at elevated temperatures, provided $\omega_c\tau$, the combination of the cyclotron frequency and the transport lifetime, is large enough. To date, expressions used to fit AMRO data have been derived assuming zero temperature, which should work reasonably well for temperatures $T \ll T_F$, the Fermi temperature. However, recently there have been relatively high temperature AMRO experiments for which corrections to the zero-temperature approximation may be needed. For instance, the experiments in Refs. 9 and 12 were performed for T up to 55 K, corresponding to a maximum thermal energy of approximately 0.02 of the Fermi energy $\varepsilon_F = k_B T_F$. At this temperature scale, one expects the zero-temperature approximation to work reasonably well in fits to AMRO. However, more recent experiments[26] have extended AMRO to temperatures as high as 110 K ($\sim 0.04 T_F$) where finite temperature effects should be more relevant—we show below that finite temperature corrections to AMRO can be quantitatively important at these temperatures.

In this paper we obtain two main results: (i) we generalize existing zero-temperature semiclassical AMRO formulae for the interlayer conductivity in layered metals with anisotropic Fermi surface properties to finite temperatures; and (ii) we establish the robustness of the fitting procedure used in Ref. 9 to finite temperature corrections. We use our expression for the interlayer conductivity [Eq. (16)] to generate numerically the AMRO expected in overdoped thallium cuprate for an isotropic scattering rate. Fitting to the simulated AMRO with zero-temperature expressions reveals no significant anisotropic contribution to the scattering rate. We find that whilst the inferred scattering rates in Ref. 9 are robust to finite temperature corrections, these corrections will be required in fits to AMRO at higher temperatures.

This paper is structured as follows: in Sec. II we present our analytic calculations of AMRO. In Sec. III we perform numerical calculations to check whether the finite temperature effects can masquerade as linear in T anisotropic scattering. In Sec. IV we summarize our results and conclude.

II. CALCULATION OF AMRO

In this section we briefly review the calculation of the interlayer conductivity in a layered metal allowing for nonzero temperature and treat the cases of isotropic Fermi surface properties (for which we can make considerable analytic progress) and anisotropic Fermi surface properties separately. We assume a simple model of a layered metal in which the c axis is the weakly conducting direction and take a dispersion relation of the form

$$\varepsilon(\mathbf{k}) = \varepsilon_{2d}(k_x,k_y) - 2t_c(k_x,k_y)\cos(ck_z), \tag{1}$$

where $\mathbf{k}=(k_x,k_y,k_z)$ is the electron wave vector, ε_{2d} is the dispersion in the k_x-k_y plane, $t_c(k_x,k_y)$ is the (possibly aniso-

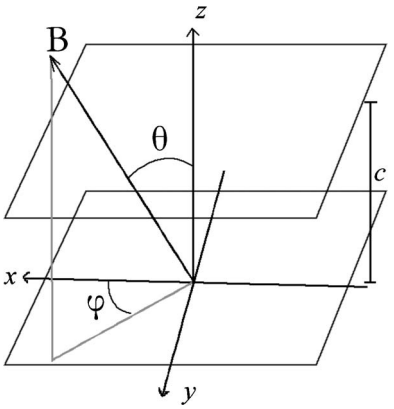

FIG. 1. Schematic of the magnetic field in an AMRO experiment. The polar angle θ is measured relative to the z axis and the azimuthal angle φ relative to the x axis, which lies in the conducting plane.

tropic) interlayer hopping term (assumed to be small compared to the Fermi energy), and the parameter c is the distance between the conducting layers.

We treat the electrons semiclassically and calculate AMRO by solving the time independent and spatially uniform Boltzmann equation in the relaxation time approximation,

$$\mathbf{F}\cdot\frac{\partial f}{\partial \mathbf{p}} = -\frac{f-f_T}{\tau}, \tag{2}$$

where $f(\mathbf{p})$ is the electron distribution function, in terms of momentum $\mathbf{p}$, f_T is the Fermi-Dirac distribution, $\mathbf{F}=-e(E_z\hat{\mathbf{z}}+\mathbf{v}\times\mathbf{B})$ is the Lorentz force for a magnetic field $\mathbf{B}$ and a weak electric field perpendicular to the conducting layers, E_z, $\mathbf{v}=\hbar^{-1}\nabla_{\mathbf{k}}\varepsilon(\mathbf{k})$ is the velocity, and τ is the transport lifetime. In general τ may depend on both the electron momentum and energy. We assume that the magnetic field $\mathbf{B}=B(\sin\theta\cos\varphi,\sin\theta\sin\varphi,\cos\theta)$ is applied at an angle θ with respect to the z axis and an angle φ with respect to the x axis, as shown schematically in Fig. 1.

For weak electric fields we can write $f\approx f_T+\delta f$, where $\delta f\sim\mathcal{O}(E_z)$. Neglecting small terms in the electric field and the hopping, t_c, we obtain

$$\frac{\partial f}{\partial \phi}+\frac{f}{\omega_0(\varepsilon,\phi)\tau(\varepsilon,\phi)} = -\frac{ev_zE_z}{\omega_0(\varepsilon,\phi)}\left(-\frac{\partial f_T}{\partial\varepsilon}\right), \tag{3}$$

where ϕ is the angular position in momentum space and ε is energy. We relabeled $\delta f\to f$ for convenience, and define[10]

$$\omega_0(\varepsilon,\phi) = eB\cos\theta\frac{\mathbf{k}_\parallel(\varepsilon,\phi)\cdot\mathbf{v}_\parallel(\varepsilon,\phi)}{\hbar|\mathbf{k}_\parallel(\varepsilon,\phi)|^2},$$

with $\mathbf{v}_\parallel=(v_x,v_y)$ and $\mathbf{k}_\parallel=(k_x,k_y)$. The in-plane dispersion relation $\varepsilon_{2d}(k_x,k_y)$ determines $\mathbf{v}_\parallel$ and $\mathbf{k}_\parallel$; accordingly, if ε_{2d} is anisotropic, $\mathbf{v}_\parallel$, $\mathbf{k}_\parallel$ and $\omega_0(\varepsilon,\phi)$ will also be anisotropic in momentum space.

Equation (3) holds for both isotropic and anisotropic Fermi surfaces. The formal solution to Eq. (3) is

$$f(\phi,\varepsilon) = -eE_z\int_0^\infty d\varepsilon\int_{-\infty}^{\phi}d\phi' G(\phi,\phi',\varepsilon)\frac{v_z(\varepsilon,\phi')}{\omega_0(\varepsilon,\phi')}\left(-\frac{\partial f_T}{\partial\varepsilon}\right), \tag{4}$$

where

$$G(\phi,\phi',\varepsilon) = \exp\left[-\int_{\phi'}^{\phi}\frac{d\psi}{\omega_0(\varepsilon,\psi)\tau(\varepsilon,\psi)}\right], \tag{5}$$

is the probability that an electron will travel around the Fermi surface from an angle ϕ' to ϕ without being scattered.[10] With this expression we may calculate the current density $j_z=-2e\int\frac{d^3\mathbf{k}}{(2\pi)^3}v_zf$ and hence the interlayer conductivity σ_{zz}. In Sec. II A and Sec. II B we present the resulting finite temperature interlayer conductivity for both isotropic and anisotropic cases, respectively.

A. Isotropic Fermi surface

We first consider finite temperature effects for an isotropic layered metal, with isotropic scattering rate $1/\tau$ (we allow τ to depend on ε and unless otherwise specified, make no assumptions about its temperature dependence), isotropic hopping t_c and an isotropic dispersion,[27]

$$\varepsilon_{2d}(k_x,k_y) = \frac{\hbar^2}{2m^*}(k_x^2+k_y^2), \tag{6}$$

where m^* is the effective mass. This gives $\omega_0=eB\cos\theta/m^*$.

In the zero-temperature limit the expression for the interlayer conductivity is[28,29]

$$\sigma_{zz}(\theta) = \sigma_0\left[J_0^2(\gamma k_F)+2\sum_{s=1}^{\infty}\frac{J_s^2(\gamma k_F)}{1+(s\omega_0\tau)^2}\right], \tag{7}$$

where $\sigma_0=\frac{2e^2m^*ct_c^2\tau}{\pi\hbar^4}$ (τ, if energy dependent, is evaluated at the Fermi energy) and $\gamma=c\tan\theta$. To generalize this expression to finite temperature we must integrate over energy in calculating σ_{zz}. The integral to be evaluated is

$$\sigma_{zz} = \vartheta_0\int_0^\infty d\varepsilon\left(-\frac{\partial f_T}{\partial\varepsilon}\right)\tau(\varepsilon)\times\left[J_0^2(\lambda\sqrt{\varepsilon})+2\sum_{s=1}^{\infty}\frac{J_s^2(\lambda\sqrt{\varepsilon})}{1+(s\omega_0\tau(\varepsilon))^2}\right], \tag{8}$$

where the energy dependence of the scattering time τ must be taken into account, $\vartheta_0=2e^2m^*ct_c^2/\pi\hbar^4$, and $\lambda=\frac{\gamma k_F}{\sqrt{\varepsilon_F}}$. Using a Sommerfeld expansion[30] and keeping terms to order $(T/T_F)^2$, we arrive at the result

$$\sigma_{zz}\simeq\vartheta_0\left\{\tau(\mu)\left\{J_0^2(\lambda\sqrt{\mu})+2\sum_{s=1}^{\infty}\frac{J_s^2(\lambda\sqrt{\mu})}{1+[s\omega_0\tau(\mu)]^2}\right\}+\frac{\pi^2}{6}(k_BT)^2\left[\Psi_0(\varepsilon_F)+2\sum_{s=1}^{\infty}\Psi_s(\varepsilon_F)\right]\right\}, \tag{9}$$

where the chemical potential is

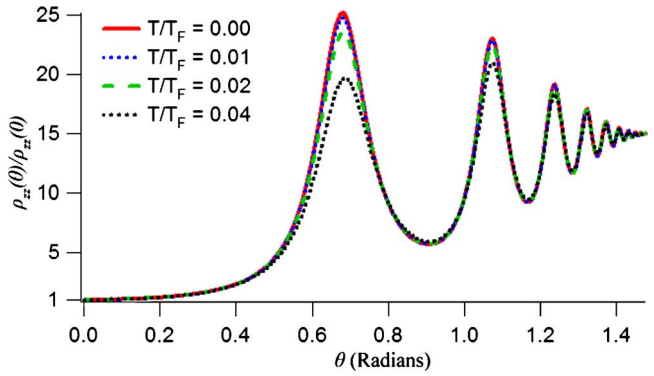

FIG. 2. (Color online) Plot of ρ_{zz}/ρ_0 versus θ for an isotropic Fermi surface with $ck_F=3$ and $\omega_c\tau=5$ at temperatures of $T/T_F=0$, 0.01, 0.02 and 0.04.

$$\mu = \varepsilon_F\left[1 - \frac{\pi^2}{12}\left(\frac{T}{T_F}\right)^2 + \cdots\right],$$

and we introduce

$$\Psi_s(\varepsilon) = \frac{d^2}{d\varepsilon^2}\left\{\tau(\varepsilon)\frac{J_s^2(\lambda\sqrt{\varepsilon})}{1+[s\omega_0\tau(\varepsilon)]^2}\right\}. \tag{10}$$

In Fig. 2 we plot the interlayer resistivity $\rho_{zz}=1/\sigma_{zz}$ (normalized by $\rho_0=1/\sigma_0$), determined from Eqs. (7) and (9) for an energy- independent τ at several different temperatures. We choose $ck_F=3$ and $\omega_c\tau=5$ (where $\omega_c=eB/m^*$) to match values used in plots in Ref. 31 and plot temperatures of 0, $0.01T_F$, $0.02T_F$, and $0.04T_F$. Deviations from the zero-temperature result are mainly noticeable in the first few AMRO peaks, for $T/T_F \gtrsim 0.02$. Interestingly, the minima seem much less affected by finite temperature than the maxima, which can be understood from arguments we present below.

To see why the maxima are affected more than minima we perform an asymptotic expansion of Eq. (9) in the limit $ck_F \tan\theta \to \infty$ for an energy independent τ. The derivation follows that for the $T=0$ case in Ref. 31. We find the correction to the zero-temperature result to be [when $(ck_F \tan\theta)(\frac{T}{T_F})^2 \ll 1$]

$$\Delta\sigma_{zz} = \frac{\vartheta_0}{ck_F\tan\theta}\frac{\pi^2}{6}\left(\frac{T}{T_F}\right)^2\frac{1}{\sinh\left(\frac{\pi}{\omega_c\tau\cos\theta}\right)} \times\left[\cosh\left(\frac{\pi}{\omega_c\tau\cos\theta}\right) + (1 - (ck_F\tan\theta)^2)\sin(2ck_F\tan\theta) - 2ck_F\tan\theta\cos(2ck_F\tan\theta)\right]. \tag{11}$$

The extrema of the resistivity occur at the Yamaji angles,[32] which satisfy

$$ck_F\tan\theta_n = \pi\left(n+\frac{\nu}{4}\right), \tag{12}$$

where $\nu=1(3)$ corresponds to a minimum (maximum) of the resistivity $\rho_{zz}=1/\sigma_{zz}$. [Note that there will be $\mathcal{O}(T^2/T_F^2)$ corrections to the Yamaji angles, although as can be seen in Fig. 2, these are not large, and they are not important for our discussion here.] The convention used here for n is that the nth minimum follows the nth maximum and n begins at zero. We can calculate the $\mathcal{O}(T^2/T_F^2)$ correction to the extrema of the resistivity using Eq. (11). We find that at maxima the relative change in the resistance is

$$\frac{\Delta\rho_{zz}^{\max}(T\neq 0)}{\rho_{zz}^{\max}(T=0)} = -\frac{\pi^2}{6}\left(\frac{T}{T_F}\right)^2\frac{1}{\cosh\left(\frac{\pi}{\omega_c\tau\cos\theta_n^{\max}}\right)-1} \times\left[\cosh\left(\frac{\pi}{\omega_c\tau\cos\theta_n^{\max}}\right) + \pi^2\left(n+\frac{3}{4}\right)^2\right], \tag{13}$$

and at minima the relative change in resistance is

$$\frac{\Delta\rho_{zz}^{\min}(T\neq 0)}{\rho_{zz}^{\min}(T=0)} = -\frac{\pi^2}{6}\left(\frac{T}{T_F}\right)^2\frac{1}{\cosh\left(\frac{\pi}{\omega_c\tau\cos\theta_n^{\min}}\right)+1} \times\left[\cosh\left(\frac{\pi}{\omega_c\tau\cos\theta_n^{\min}}\right) - \pi^2\left(n+\frac{1}{4}\right)^2\right]. \tag{14}$$

In general the numerators in the two expressions will be comparable, but the denominator in the minima expression is always greater than 2, whereas the denominator in the maxima expression can become very small when $\omega_c\tau\cos\theta_n^{\max}$ becomes large, leading to a much stronger reduction in the resistance at the maxima than increase at the resistance minima. [It should be noted that assuming temperature independent scattering, as we do in this example, is somewhat artificial. In general one expects the scattering rate to have a T^2 contribution at low temperatures from electron-electron scattering in a Fermi liquid, along with contributions from electron-phonon scattering and scattering of electrons off disorder, which will generically have different temperature dependences. We ignore these details in this section to better illustrate the differing effects of temperature on resistance minima and maxima, but they need to be taken into account in fitting transport data in experiment.]

B. Anisotropic Fermi surface

We now turn to consider finite temperature effects for an anisotropic Fermi surface. We allow ω_0, τ, $\mathbf{v}_\parallel$, $\mathbf{k}_\parallel$, and t_c to vary with ϕ and ε. The zero-temperature interlayer conductivity for a layered metal with anisotropic Fermi surface properties was calculated by Kennett and McKenzie[10] to be

$$\sigma_{zz} = \frac{s_0 eB\cos\theta}{1-P}\int_0^{2\pi} d\phi \int_{\phi-2\pi}^{\phi} d\phi' \times \frac{t_c(\phi)t_c(\phi')}{\omega_0(\phi)\omega_0(\phi')} G(\phi,\phi',\varepsilon_F)\cos\Phi(\phi,\phi'), \quad (15)$$

where $s_0 = e^2c/(\pi\hbar^4)$, $P = G(2\pi,0,\varepsilon_F)$ is the probability that an electron will make a full cyclotron orbit about the Fermi surface before being scattered and

$$\Phi(\phi,\phi') = \gamma\hat{\mathbf{b}}_\parallel(\varphi)\cdot[\mathbf{k}_F(\phi)-\mathbf{k}_F(\phi')] = \gamma[k_F(\phi)\cos(\varphi-\phi)-k_F(\phi')\cos(\varphi-\phi')],$$

where we have defined $\hat{\mathbf{b}}_\parallel(\varphi)=(\cos\varphi,\sin\varphi)$ as the direction of the component of the magnetic field in the x-y plane, and $\mathbf{k}_F(\phi)=k_F(\phi)(\cos\phi,\sin\phi)$, where $k_F(\phi)$ is the magnitude of the Fermi wave vector.

Generalizing Eq. (15) for the interlayer conductivity to finite temperatures is similar to the isotropic case, and again we integrate over energy,

$$\sigma_{zz} = s_0 eB\cos\theta\int_{-\infty}^{\infty} d\varepsilon\int_0^{2\pi} d\phi\int_{\phi-2\pi}^{\phi} d\phi' \times\left(-\frac{\partial f_T}{\partial\varepsilon}\right)\frac{t_c(\varepsilon,\phi)t_c(\varepsilon,\phi')}{\omega_0(\varepsilon,\phi)\omega_0(\varepsilon,\phi')}\frac{G(\phi,\phi',\varepsilon)}{1-P(\varepsilon)}\cos\Phi(\phi,\phi',\varepsilon). \quad (16)$$

The factor $G(\phi,\phi',\varepsilon)$ is as in Eq. (5), and the energy-dependent $\Phi(\phi,\phi',\varepsilon)$ is

$$\Phi(\phi,\phi',\varepsilon) = \gamma[\kappa(\varepsilon,\phi)\cos(\varphi-\phi)-\kappa(\varepsilon,\phi')\cos(\varphi-\phi')], \quad (17)$$

where $\kappa(\varepsilon,\phi)\equiv|\mathbf{k}_\parallel|=\sqrt{k_x^2+k_y^2}$ is the magnitude of the electron wave vector. Allowed values of κ are determined from the dispersion relation. Equation (16) is our main result and is independent of whether the interlayer hopping is coherent (assumed here) or weakly incoherent.[10,28,31] The only difference in AMRO for the two models of transport occurs for angles near $\theta=\frac{\pi}{2}$.[1,28,31,33]

In order to make analytic progress with Eq. (16) we need to specify the energy and ϕ dependence of various Fermi surface properties. In general, AMRO must be calculated numerically, although under certain conditions we may derive asymptotic expressions. To do so, we note that if ω_0 never approaches zero, the largest contribution to the integrand of Eq. (16) will be from near $\varepsilon=\mu$, where the derivative of the Fermi-Dirac function is sharply peaked. We can then perform a Sommerfeld expansion about this point, as in the isotropic finite temperature case. The zeroth order term gives the zero-temperature result evaluated at μ instead of ε_F. Under the conditions

$$c\kappa(\mu,\phi)\tan\theta \gg 1, \quad \frac{eBc|\mathbf{v}_\parallel(\mu,\phi)|\tau(\mu,\phi)}{\hbar} \gg 1,$$

we can evaluate the zeroth order term using a stationary phase calculation.[10] To second order in T/T_F we can then write the temperature dependent conductivity, valid near $\theta=\frac{\pi}{2}$, for a Fermi surface with $\phi\to\phi+\frac{\pi}{2}$ symmetry as

$$\sigma_{zz}(\theta,\varphi,T) \simeq \frac{eBs_0\cos\theta}{1-P(\mu)}\frac{2\pi|\eta(\mu,\phi_0)|^{-1}}{c\tan\theta}\left(\frac{t_c(\mu,\phi_0)}{\omega_0(\mu,\phi_0)}\right)^2 \times[1+P(\mu)+2\sqrt{P(\mu)}\sin(2c\tan\theta\kappa(\mu,\phi_0) \times\cos(\varphi-\phi_0))]+\frac{\pi^2}{6}eBs_0\cos\theta(k_BT)^2\Omega(\varepsilon_F), \quad (18)$$

where ϕ_0 satisfies $\frac{\partial}{\partial\phi}[\hat{\mathbf{b}}_\parallel(\varphi)\cdot\mathbf{k}_\parallel(\varepsilon,\phi)]=0$, $\eta(\varepsilon,\phi)\equiv\frac{\partial^2}{\partial\phi^2}[\hat{\mathbf{b}}_\parallel(\varphi)\cdot\mathbf{k}_\parallel(\phi)]$, and

$$\Omega(\varepsilon) = \frac{d^2}{d\varepsilon^2}\left[\int_0^{2\pi} d\phi\int_{\phi-2\pi}^{\phi} d\phi'\frac{t_c(\varepsilon,\phi)t_c(\varepsilon,\phi')}{\omega_0(\varepsilon,\phi)\omega_0(\varepsilon,\phi')}\frac{G(\phi,\phi',\varepsilon)}{1-P(\varepsilon)}\cos\Phi(\phi,\phi',\varepsilon)\right] \simeq \frac{eBs_0\cos\theta}{c\tan\theta}\frac{d^2}{d\varepsilon^2}\left\{\frac{2\pi|\eta(\varepsilon,\phi_0)|^{-1}}{1-P(\varepsilon)}\left(\frac{t_c(\varepsilon,\phi_0)}{\omega_0(\varepsilon,\phi_0)}\right)^2[1+P(\varepsilon)+2\sqrt{P(\varepsilon)}\sin(2c\tan\theta\kappa(\varepsilon,\phi_0)\cos(\varphi-\phi_0))]\right\}. \quad (19)$$

III. NUMERICS

We now outline the numerical scheme we use to test whether the temperature dependence of the conductivity affects the anisotropy obtained from fits to the scattering rate $1/\tau$ using zero-temperature expressions for the conductivity. Our approach is as follows: we use the tight-binding dispersion relation inferred for Tl2201 from ARPES (Ref. 18) to simulate the AMRO data we expect to observe at several different temperatures and azimuthal field angles φ, assuming an isotropic scattering rate of the form predicted by Fermi liquid theory. We then fit to this data using the same procedure used to fit experimental data in Ref. 9. First, we allow all parameters to vary in fitting the lowest temperature data (using the zero-temperature expression for the interlayer resistivity). Second, the higher temperature data is fitted assuming only the scattering rate is temperature dependent. If the scattering rate anisotropy is a fitting artifact, fits to AMRO data simulated with finite temperature expressions for the conductivity should yield results similar to the fits to the real data: an anisotropic contribution to the scattering rate

TABLE I. Fitting parameters for $\kappa(\varepsilon,\phi)$ and $1/\omega_0(\varepsilon,\phi)$.

	$1/\omega_{00}$	$1/\omega_{01}$	$1/\omega_{02}$	$1/\omega_{03}$	κ_0	κ_1	κ_2
C_0	4.768	−0.582	0.035	0.035	1.786	−0.077	0.002
C_1	8.097	2.670	−1.388	−0.361	1.039	0.025	−0.030

that varies as $T\cos 4\phi$. Finally, we include the anisotropic component of the scattering inferred in Ref. 9 and test that it is indeed found in the fitting procedure. This is in some sense a more stringent test of the fitting procedure than actually fitting experimental data, as we know all of the appropriate parameters that should be determined in the fitting procedure, whereas in experiment, the exact underlying parameters are unknown.

The tight binding dispersion relation determined by Platé *et al.*[18] is

$$\begin{aligned}\varepsilon_{2d}(k_x,k_y) = \mu + \frac{t_1}{2}(\cos k_x + \cos k_y) + t_2(\cos k_x \cos k_y) \\ + \frac{t_3}{2}(\cos 2k_x + \cos 2k_y) + \frac{t_4}{2}(\cos 2k_x \cos k_y \\ + \cos k_x \cos 2k_y + \cos k_x \cos k_y) \\ + t_5 \cos 2k_x \cos 2k_y, \end{aligned} \tag{20}$$

where the wave numbers are measured in units of the in-plane lattice constant a, the t_i are hopping parameters and μ is the chemical potential. The values of the parameters are $\mu=0.2438$, $t_1=-0.725$, $t_2=0.302$, $t_3=0.0159$, $t_4=-0.0805$, and $t_5=0.0034$, all in eV. We use ε_{2d} to calculate $1/\omega_0$ and κ as functions of ϕ numerically, for several energies, where we consider the hole Fermi surface centered on (π,π). We fit the output data to give a functional form of $1/\omega_0$ and κ as functions of ϕ and ε.

The Fermi surface for the dispersion Eq. (20) exhibits a $\phi\rightarrow\phi+\frac{\pi}{2}$ symmetry, and so $\kappa(\varepsilon,\phi)$ and $1/\omega_0(\varepsilon,\phi)$ also have this symmetry. This allows us to fit the data to a truncated Fourier series with only $\cos 4n\phi$, $n\in\mathbb{Z}$, terms present.[2,6] We find that $1/\omega_0(\varepsilon,\phi)$ may be accurately represented by the form

$$\begin{aligned}\frac{1}{\omega_0(\varepsilon,\phi)} = \frac{1}{\omega_{00}(\varepsilon)} + \frac{1}{\omega_{01}(\varepsilon)}\cos 4\phi + \frac{1}{\omega_{02}(\varepsilon)}\cos 8\phi \\ + \frac{1}{\omega_{03}(\varepsilon)}\cos 12\phi \end{aligned} \tag{21}$$

and $\kappa(\varepsilon,\phi)$ may be parametrized as

$$\kappa(\varepsilon,\phi) = \kappa_0(\varepsilon) + \kappa_1(\varepsilon)\cos 4\phi + \kappa_2(\varepsilon)\cos 8\phi. \tag{22}$$

For the energy range we are interested in the energy dependence of each of the coefficients can be well approximated as linear, $C(\varepsilon)=C_0+C_1\varepsilon$. Contributions to the integral [Eq. (16)] from energies far from the Fermi energy are negligible. In our simulations we use the combination $c\kappa(\varepsilon_F)=ck_F=8.64$. The fitting parameters for κ and $1/\omega_0$ are given in Table I.

The remaining functional inputs we need to calculate the AMRO are the interlayer hopping $t_c(\phi)$ and the scattering rate $1/\tau(\varepsilon,\phi)$. We assume the standard isotropic scattering rate for $1/\tau(\varepsilon)$,[34,35]

$$\frac{1}{\tau} = \frac{1}{\tau_0} + A[(\pi k_B T)^2 + (\varepsilon-\mu)^2]. \tag{23}$$

We estimate the parameters $1/\tau_0$ and A for $1/\tau$ from fits to the isotropic part of the scattering rate in Ref. 9, giving $A=(13.5\ \text{meV})^{-2}$; $1/\tau_0$ always appears as part of a product $1/\omega_0(\varepsilon_F)\tau_0$, where $1/\omega_0(\varepsilon_F)$ is the constant contribution to $1/\omega_0(\varepsilon,\phi)$ at the Fermi energy, and we find that $1/\omega_0(\varepsilon_F)\tau_0=2.5$. We assume the hopping is independent of energy and use the same expression for the hopping term as in Ref. 10,

$$t_c(\phi) = t_0[\sin 2\phi + \eta_1 \sin 6\phi + \eta_2 \sin 10\phi]. \tag{24}$$

The parameters η_1 and η_2 are related to each other by the symmetry of the crystal lattice, which requires $t_c(\phi)=-t_c(\phi+\frac{\pi}{2})$ and hence $\eta_1=1+\eta_2$. Due to imperfections in the crystal, this relation may not hold exactly, and we allow both parameters to vary during fitting. The input values are $\eta_1=0.737$ and $\eta_2=-0.263$. The constant t_0 enters the overall normalization and does not need to be specified in our calculation.

With explicit functional forms for all functions appearing in Eq. (16), we may perform the angular and energy integrals. Due to the fact that the derivative of the Fermi function decays quickly away from $\varepsilon=\mu$ we only integrate over the energy from $\mu-5k_BT$ to $\mu+5k_BT$ to cover the range of energy that contributes to the integral, and we checked that our results were independent of the energy range for this choice of integration interval. The values of φ we use are 0, 20, 28, 36, and 44 degrees and we generate AMRO for $T=0.001T_F-0.04T_F$, where T_F is $\mathcal{O}(3000\ \text{K})$. These correspond to temperatures from 3 to 113 K. The output is normalized such that $\rho_{zz}(\theta=0)=1$. The simulated AMRO data are shown in Fig. 3.

Fitting the simulated data

We fit to the simulated AMRO data using Eq. (24) for $t_c(\phi)$ and parameterize the scattering rate as[9,10]

$$\frac{1}{\tau(\phi)} = \frac{1}{\tau}[1+\alpha\cos 4\phi]. \tag{25}$$

The Fermi wave vector and cyclotron frequency are parametrized as

$$k_F(\phi) = k_F[1+k_4\cos 4\phi], \tag{26}$$

and

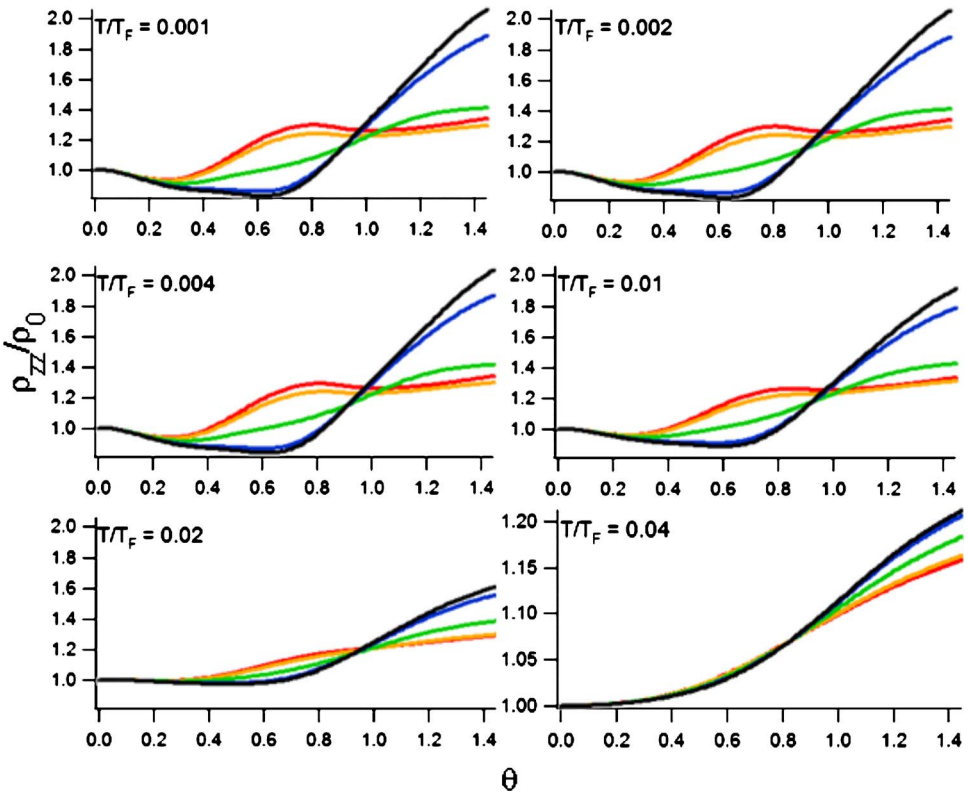

FIG. 3. (Color online) AMRO data calculated numerically using paramters appropriate for thallium cuprate, assuming isotropic scattering. The values of φ used are 0°, 20°, 28°, 36° and 44°. Note the change in vertical axis limits in the last plot. The plots shown correspond to temperatures of 2.8, 5.7, 11.3, 28, 56, and 113 K.

$$\frac{1}{\omega_0(\phi)} = \frac{1}{\omega_{00}}[1 + u\cos 4\phi]. \tag{27}$$

We use the 2.8 K data to fit to the parameters α, k_4, u, $\omega_{00}\tau$, ck_F, η_1, and η_2. For fits at temperatures above 2.8 K we assume that only the scattering rate is temperature dependent, and fit only to the parameters $\omega_{00}\tau$ and α. The scattering rate parameters $1/\omega_{00}\tau$ and $\alpha/\omega_{00}\tau$ are plotted as a function of temperature in Fig. 4. A quadratic fit $a[1+(b\pi k_B T)^2]$ to $1/\omega_{00}\tau$ yields $a=2.49$ and $\pi k_B b = 51$ K^{-1}, agreeing with the parameter values used to simulate the AMRO. The fit values obtained are $k_4=-0.025$, $u=-0.153$, $ck_F=8.607$, $\eta_1=0.764$, and $\eta_2=-0.245$, which are within 1–2 % of the input parameter values used in the simulation.

We find that not only do the fits to the simulated data fail to reproduce the $T\cos 4\phi$ term observed in the experiments, we observe essentially no temperature dependence of the anisotropy parameter α, suggesting that if the scattering rate were in fact isotropic the fitting procedure used by Abdel-Jawad *et al.*[9] would not have yielded anisotropic scattering. Hence, the anisotropic contribution to the electron-electron scattering rate measured in recent AMRO experiments is not an artifact of the fitting procedure, and the system does deviate from standard Fermi liquid behavior.

As a further comparison to the experiment in Ref. 9, we simulated AMRO including anisotropy in the scattering. The AMRO were generated exactly as above, except that we took α to be

$$\frac{\alpha}{\omega_{00}\tau} = -0.154 + \frac{T}{32.5},$$

as determined from Ref. 9. Note that unlike the isotropic piece of the scattering, where we included Fermi liquidlike energy dependence we took this term to be energy independent, since its origin (and energy dependence) are not well established. The Fermi surface parameters we found from fitting the AMRO were $k_4=-0.028$, $u=-0.152$, $ck_F=8.598$, $\eta_1=0.747$, $\eta_2=-0.257$ which are in good agreement with those found above for isotropic scattering. In Fig. 5 we display the variation of $1/\omega_{00}\tau$ and $\alpha/\omega_{00}\tau$ with temperature and compare them to the values found in Ref. 9 that were

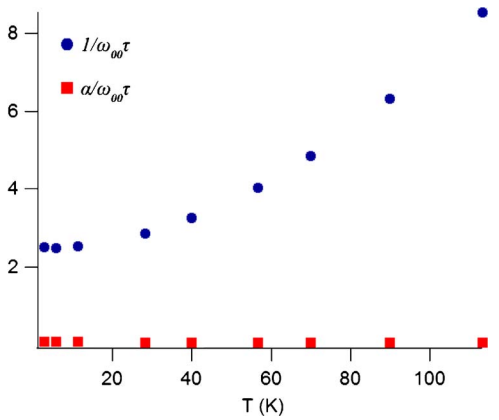

FIG. 4. (Color online) Plot of fit parameters $1/\omega_{00}\tau$ and $\alpha/\omega_{00}\tau$ as functions of temperature.

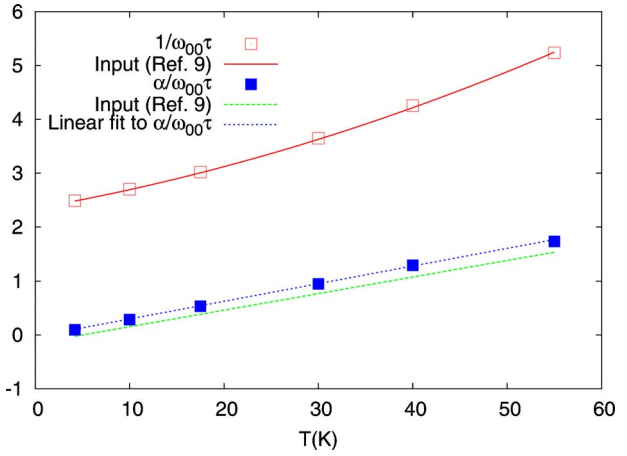

FIG. 5. (Color online) Plot of fit parameters $1/\omega_{00}\tau$ and $\alpha/\omega_{00}\tau$ as functions of temperature when anisotropy in the scattering is included in the simulated AMRO.

used as input. Apart from a slight shift in the $T=0$ intercept of α as a function of temperature from the input—the best fit line is $\alpha/\omega_{00}\tau=-0.03+T/30.5$, the linear trend with temperature is very much in evidence, with a very similar slope to the input, in strong contrast to the essentially temperature independent α in Fig. 4 above.

IV. CONCLUSIONS

In this work we presented expressions for the interlayer conductivity of layered metals with either an isotropic or anisotropic Fermi surface, allowing for thermal effects. We used the expression for the conductivity for a layered metal with anisotropic Fermi surface properties to simulate the AMRO expected an isotropic scattering rate consistent with Fermi liquid theory. Fitting to the simulated data using the same procedure used to fit the experimental data in Ref. 9 does not reproduce the anisotropic $T\cos 4\phi$ piece of the scattering rate. However, when anisotropic scattering is included as an input to the simulated AMRO, the inferred scattering rate is essentially the same as that included in the simulation. Hence, we have confirmed that including finite temperature effects whilst taking into account anisotropy in the dispersion does not affect the conclusion that there is an anisotropic contribution to the scattering rate of thallium cuprate.

The theory presented here is applicable to any layered metal in which AMRO may be observed, and provides the means to analyze AMRO data for temperatures at which T/T_F grows large enough that finite temperature effects on AMRO become significant. In Sec. II A we observed that for $T/T_F \gtrsim 0.02$, finite temperature corrections to AMRO appear to be important. This estimate is based on considering the idealized situation of an isotropic dispersion with isotropic temperature independent scattering and is mainly meant to give a guide as to where one should be careful in fitting experimental data—we anticipate that in most cases anisotropy effects should not change our estimate by more than factors of order unity. Having a threshold above which there is an expectation of finite temperature corrections may allow for a more precise interpretation of current AMRO data at higher temperatures, for example in cuprate experiments[26] where the maximum value of T/T_F is $\sim 0.03-0.04$ or in $Na_{0.48}CoO_2$, which has a Fermi energy around 250 meV,[36] and AMRO experiments have been performed at temperatures as high as $T/T_F \sim 0.02$.[37] This theory will also enable accurate quantitative analysis of future high temperature AMRO experiments.

ACKNOWLEDGMENTS

We thank R. McKenzie and N. Hussey for helpful discussions on AMRO. This work was supported by NSERC.

[1] M. V. Kartsovnik, Chem. Rev. **104**, 5737 (2004).
[2] C. Bergemann, A. P. Mackenzie, S. R. Julian, D. Forsythe, and E. Ohmichi, Adv. Phys. **52**, 639 (2003).
[3] L. Balicas, S. Nakatsuji, D. Hall, T. Ohnishi, Z. Fisk, Y. Maeno, and D. J. Singh, Phys. Rev. Lett. **95**, 196407 (2005).
[4] T. Osada, H. Nose, and M. Kuraguchi, Physica B **294-295**, 402 (2001).
[5] U. Beierlein, C. Schlenker, J. Dumas, and M. Greenblatt, Phys. Rev. B **67**, 235110 (2003).
[6] N. E. Hussey, M. Abdel-Jawad, A. Carrington, A. P. Mackenzie, and L. Balicas, Nature (London) **425**, 814 (2003).
[7] K. Enomoto, S. Uji, T. Yamaguchi, T. Terashima, T. Konoike, M. Nishimura, T. Enoki, M. Suzuki, and I. S. Suzuki, Phys. Rev. B **73**, 045115 (2006).
[8] K. G. Sandeman and A. J. Schofield, Phys. Rev. B **63**, 094510 (2001).
[9] M. Abdel-Jawad, M. P. Kennett, L. Balicas, A. Carrington, A. P. Mackenzie, R. H. McKenzie, and N. E. Hussey, Nat. Phys. **2**, 821 (2006).
[10] M. P. Kennett and R. H. McKenzie, Phys. Rev. B **76**, 054515 (2007).
[11] M. Abdel-Jawad, J. G. Analytis, L. Balicas, A. Carrington, J. P. H. Charmant, M. M. J. French, and N. E. Hussey, Phys. Rev. Lett. **99**, 107002 (2007).
[12] J. G. Analytis, M. Abdel-Jawad, L. Balicas, M. M. J. French, and N. E. Hussey, Phys. Rev. B **76**, 104523 (2007).
[13] M. P. Kennett and R. H. McKenzie, Physica B **403**, 1552 (2008).
[14] N. E. Hussey, M. Abdel-Jawad, L. Balicas, M. P. Kennett, and R. H. McKenzie, Physica B **403**, 982 (2008).
[15] J. Singleton, P. A. Goddard, A. Ardavan, A. I. Coldea, S. J. Blundell, R. D. McDonald, S. Tozer, and J. A. Schlueter, Phys. Rev. Lett. **99**, 027004 (2007).
[16] M. F. Smith and R. H. McKenzie, Phys. Rev. B **77**, 235123 (2008); M. F. Smith and R. H. McKenzie, arXiv:0906.1015 (unpublished).
[17] T. Kondo, T. Takeuchi, S. Tsuda, and S. Shin, Phys. Rev. B **74**,

224511 (2006).
[18] M. Platé, J. D. F. Mottershead, I. S. Elfimov, D. C. Peets, R. Liang, D. A. Bonn, W. N. Hardy, S. Chiuzbaian, M. Falub, M. Shi, L. Patthey, and A. Damascelli, Phys. Rev. Lett. **95**, 077001 (2005); D. C. Peets, J. P. F. Mottershead, B. Wu, I. S. Elfimov, R. Liang, W. N. Hardy, D. A. Bonn, M. Raudsepp, N. J. C. Ingle, and A. Damascelli, New J. Phys. **9**, 28 (2007).
[19] A. Kaminski, H. M. Fretwell, M. R. Norman, M. Randeria, S. Rosenkranz, U. Chatterjee, J. C. Campuzano, J. Mesot, T. Sato, T. Takahashi, T. Terashima, M. Takano, K. Kadowaki, Z. Z. Li, and H. Raffy, Phys. Rev. B **71**, 014517 (2005).
[20] J. Chang, M. Shi, S. Pailhés, M. Mansson, T. Claesson, O. Tjernberg, A. Bendounan, Y. Sassa, L. Patthey, N. Momono, M. Oda, M. Ido, S. Guerrero, C. Mudry, and J. Mesot, Phys. Rev. B **78**, 205103 (2008).
[21] N. E. Hussey, J. C. Alexander, and R. A. Cooper, Phys. Rev. B **74**, 214508 (2006).
[22] A. Narduzzo, G. Albert, M. M. J. French, N. Mangkorntong, M. Nohara, H. Takagi, and N. E. Hussey, Phys. Rev. B **77**, 220502(R) (2008).
[23] L. B. Ioffe and A. J. Millis, Phys. Rev. B **58**, 11631 (1998).
[24] M. Civelli, M. Capone, S. S. Kancharla, O. Parcollet, and G. Kotliar, Phys. Rev. Lett. **95**, 106402 (2005).
[25] M. Ossadnik, C. Honerkamp, T. M. Rice, and M. Sigrist, Phys. Rev. Lett. **101**, 256405 (2008).
[26] M. M. J. French, J. G. Analytis, A. Carrington, L. Balicas, and N. E. Hussey, N. J. Phys. **11**, 055057 (2009).
[27] For the purposes of illustration we ignore possible energy dependence of the interlayer hopping t_c for an isotropic Fermi surface, but we do include this possibility in our more general analysis of a layered metal with anisotropic Fermi surface properties.
[28] R. H. McKenzie and P. Moses, Phys. Rev. Lett. **81**, 4492 (1998).
[29] R. Yagi, Y. Iye, T. Osada, and S. Kagoshima, J. Phys. Soc. Jpn. **59**, 3069 (1990).
[30] N. W. Ashcroft and N. D. Mermin, *Solid State Physics* (Saunders, Philadelphia, 1976).
[31] P. Moses and R. H. McKenzie, Phys. Rev. B **60**, 7998 (1999).
[32] K. Yamaji, J. Phys. Soc. Jpn. **58**, 1520 (1989).
[33] M. P. Kennett and R. H. McKenzie, Phys. Rev. B **78**, 024506 (2008).
[34] J. Rammer, *Quantum Transport Theory* (Perseus, Reading, MA, 1998).
[35] A. A. Abrikosov, L. P. Gorkov, and I. E. Dzyaloshinski, *Methods of Quantum Field Theory in Statistical Physics* (Dover Publications, Inc., New York, 1963).
[36] D. Qian, L. Wray, D. Hsieh, L. Viciu, R. J. Cava, J. L. Luo, D. Wu, N. L. Wang, and M. Z. Hasan, Phys. Rev. Lett. **97**, 186405 (2006).
[37] F. Hu, G. T. Liu, J. L. Luo, D. Wu, N. L. Wang, and T. Xiang, Phys. Rev. B **73**, 212414 (2006).